

Frascati Physics Series Vol. nnn (2001), pp. 000-000

HEAVY QUARKS AT FIXED TARGET - Rio de Janeiro, Oct. 9-19, 2000

CP Violation at CDF

Joseph Boudreau

University Of Pittsburgh and Fermi National Accelerator Laboratory

For the CDF Collaboration

ABSTRACT

A major goal of experimental particle physics over the next decade is to measure the sides and angles of the Unitarity triangle redundantly, and as precisely as possible. Overconstraining the triangle will test the Cabbibo-Kobayashi-Maskawa model of quark mixing. The CDF collaboration, due to begin a second run in March 2001 with major upgrades to both the accelerator and the detector, will study the angle β using B^0 decays, the angle γ using B^0 and B_s^0 decays, and a side of the triangle through the observation of $B_s^0 - \bar{B}_s^0$ mixing. Projected sensitivities are driven mostly by previous measurements using data from the first run. One highlight of the Run I B physics program is a measurement of the CP violating parameter $\sin 2\beta = 0.79_{-0.44}^{+0.41}$, based on a tagged sample of 400 B^0 decays in the mode $B^0/\bar{B}^0 \rightarrow J/\psi K_s^0$. The technology of flavor tagging, used here as well as in numerous $B^0 - \bar{B}^0$ mixing analyses in run I, is crucial and will be augmented in Run II with better particle identification capabilities. Exclusive all-hadronic final states will enter the data sample in Run II through a new displaced track trigger.

1 Introduction

A small amount of CP violation in the neutral kaon system observed in 1964¹⁾ is still the only experimentally observed violation of the symmetry between particles and antiparticles. In the framework of the standard model the source of this asymmetry is the weak interaction. The matrix relating weak interaction eigenstates to mass eigenstates is the unitary CKM matrix:

$$V_{CKM} = \begin{pmatrix} V_{ud} & V_{us} & V_{ub} \\ V_{cd} & V_{cs} & V_{cb} \\ V_{td} & V_{ts} & V_{tb} \end{pmatrix} = \begin{pmatrix} 1 - \frac{\lambda^2}{2} & \lambda & A\lambda^3(\rho + i\eta) \\ -\lambda & 1 - \frac{\lambda^2}{2} & -A\lambda^2 \\ A\lambda^3(1 - \rho - i\eta) & -A\lambda^2 & 1 \end{pmatrix} \quad (1)$$

where the second form of the matrix is an approximation due to Wolfenstein²⁾, accurate to order λ^3 , where $\lambda = \sin\theta_c$. CP violation arises due to irreducible phases in the CKM matrix unless $\eta = 0$. In this parameterization, they appear in V_{td} and V_{ub} , the elements connecting the first and third generations. A prediction of the CKM model of CP violation is that the mixing amongst generations is not arbitrary, but constrained by the unitarity of the matrix. The most poorly known elements of the CKM matrix are those connecting the first and third generations. The conditions of unitarity require

$$V_{tb}^*V_{td} + V_{cb}^*V_{cd} + V_{ub}^*V_{ud} = 1 \quad (2)$$

This constraint has a popular graphical representation, the unitarity triangle, shown in Fig. 1. The angles β and γ are the phases of the CKM matrix elements V_{ub} and V_{td} ; in the standard model they are expected to be large. The length

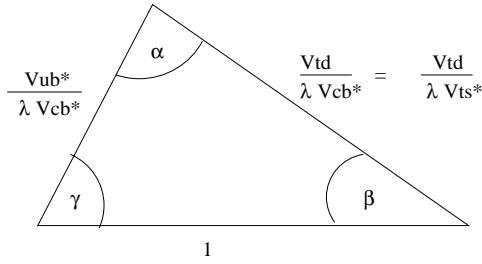


Figure 1: The (rescaled) unitarity triangle. In equation 2, divide by $V_{cb}^*V_{cd} = \lambda V_{cb}^*$ and use $V_{cb} \approx V_{ts}$.

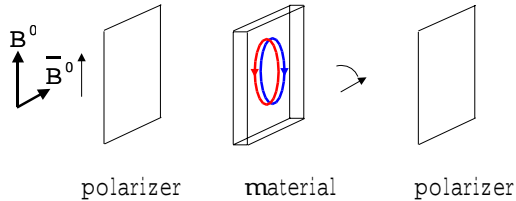


Figure 2: Example of a optical experiments analogous to B mixing and CP asymmetry experiments. In both cases the role of initial state flavor tagging is played by a linear polarizer that can single out “ B^0 ” or “ \bar{B}^0 ” polarization states. In the middle a birefringent material, with or without spatial orientation. Linear or circular polarization filters can be applied to the beam after it traverses the material.

of the right-hand side of the triangle depends upon the ratio $|V_{td}|/|V_{ts}|$, which can be determined precisely by measuring both frequencies Δm_d and Δm_s of $B^0 - \bar{B}^0$ and $B_s^0 - \bar{B}_s^0$ oscillations.

The present round of experiments is a vast program to decide whether the magnitudes and phases of V_{td} and V_{ub} respect or do not respect unitarity. As the program progresses it will mostly be discussed in terms of the geometry of the unitary triangle. The principle experimental results to be translated into this language are the measurement of the $B_s^0 - \bar{B}_s^0$ flavor oscillations, and the measurement of CP asymmetries in neutral B mesons, both B^0 and B_s^0 .

2 Time Dependent Mixing and CP asymmetries

Experimental elements of mixing and CP phenomenology, may be described by analogy to the optical phenomena of Faraday rotation, which refers to the rotation of the plane of polarization of light. An example is shown in Fig. 2, in which a beam of light passes through optical filters. The plane perpendicular to the propagation direction has two directions which we can think of as “ B^0 ” and “ \bar{B}^0 ”. The experiment consists of a polarization filter at one end of the apparatus (the “initial state flavor tag” polarizer) and a polarizer at the other other end of the detector (the “final state flavor tag” polarizer) and between them, a material which is birefringent.

One can distinguish two kinds of birefringence. The first kind singles out

no special direction in the transverse plane. Right and left handed circular polarization states travel with different speeds through the material, as in sugar solutions, where the random orientation of sugar molecules makes the material isotropic, but molecular “handedness” produces birefringence. The second kind, exhibited by certain crystalline solids, breaks the rotation symmetry in the transverse plane: the two *linear* polarizations have different propagation speeds through the medium, as in a calcite crystal.

The initial state polarizer is adjusted to admit the vertical polarization state, a superposition of left- and right- circular polarization, which travel at different speeds in a sugar solution. The two components advance in the solution with different speeds; when they recombine outside of the material, they pick up a relative phase. The resulting polarization is rotated with respect to the original, and the effect is visible with the final filter. This is analogous to B mixing; where flavor tagging plays the role of the first polarizer, while flavor-specific decay modes play the role of the second polarizer. The time-dependent $B^0 - \bar{B}^0$ flavor oscillations are demonstrated in many experiments, perhaps most exquisitely now by the BaBar ³⁾ and Belle experiments ⁴⁾.

A material that transmits distinct linear polarization states at different speeds can be regarded as a device for rotating left-circularly polarized light into right-circularly polarized light, and vice versa. Used in this optical experiment, it causes circular polarization to vary harmonically through the material. The effect can be observed by replacing the final linear polarization filter with a circular polarization filter.

The analog of the final circular polarization filter in a CP asymmetry measurement is a CP eigenstate, such as $J/\psi K_s^0$. The connection is the following. Mass eigenstates of the neutral (B^0, \bar{B}^0) system are $B_{L,H} = p|B^0 \rangle \pm q|\bar{B}^0 \rangle$. If p and q are not unity, then the mass eigenstates of the two-state system are not the CP eigenstates. As the CP mixture develops in time, so does the overlap of the meson with the final state, $J/\psi K_s^0$, which is CP odd. The CP-odd component of states that are born as \bar{B}^0 initially increases, whereas that of B^0 initially decreases. The CP asymmetry,

$$A_{CP}(t) = \frac{N(\bar{B}^0) - N(B^0)}{N(\bar{B}^0) + N(B^0)} \quad (3)$$

is sinusoidal.

In the optical analogy the explanation for the effect is of course that

the light has traveled through a crystal lattice which breaks symmetry in the transverse plane. In the quantum mechanical phenomena of CP asymmetries in the decay of $B^0/\bar{B}^0 \rightarrow J/\psi K_s^0$, the effect is predicted in the three-generation CKM model. If the model is correct, the CP asymmetry is

$$A_{CP}(t) = \frac{N(\bar{B}^0) - N(B^0)}{N(\bar{B}^0) + N(B^0)} = \sin 2\beta \sin \Delta m_d t \quad (4)$$

where β is the phase of V_{td} .

The initial state flavor tagging in a proton machine, has a low analyzing power. The figure of merit is the product of the efficiency ϵ with the square of the dilution $D = 2P - 1$, or ϵD^2 . Whereas e^+e^- machines typically achieve 30%, in $p\bar{p}$ events we have only achieved about 6%; however this is compensated by a higher cross section, approximately $50 \mu b$. The actual flavor-tagging is a combination of three flavor-tagging algorithms called same-side tagging, jet-charge tagging, and soft-lepton tagging, discussed more fully below. Like the optical Gdanken-experiments, in real life we perform mixing analyses *and* CP violation analyses using the same initial-state flavor tagging technology and changing only the final state from a flavor specific decay to a CP eigenstate, analogous to swapping a linear polarizer with a circular polarizer.

3 Run I measurement of $\sin 2\beta$

The CDF Run I measurement of $\sin 2\beta$ ⁶⁾ is an extraction of the amplitude of the CP asymmetry in the decay $B^0/\bar{B}^0 \rightarrow J/\psi K_s^0$, performed with approximately 400 fully reconstructed decays and an effective tagging efficiency of about 6%. The CDF detector has been described elsewhere ⁵⁾. The decays entered primarily through the J/ψ trigger, which requires two stubs in the muon detectors for a level one trigger decision, and for the level-two trigger decision requires a track in the Central Tracking Chamber(CTC) with $p_T > 2.0$ GeV, matching the muon stub, and satisfying an invariant mass cut $2.8 \text{ GeV} < m_{\mu\mu} < 3.4 \text{ GeV}$. This trigger results in a clean sample of 440,000 J/ψ 's in 110 pb^{-1} of data, about 20% from B decays.

The signal is reconstructed by requiring each muon from the J/ψ candidate to have $p_T > 1.4$ GeV and a K_s^0 candidate reconstructed in $K_s^0 \rightarrow \pi^+\pi^-$ to have $p_T > 700$ MeV and $L_{xy}/\sigma_{xy} > 5.0$, where L_{xy} and σ_{xy} are the transverse decay length and its error. A four particle vertex fit is performed using

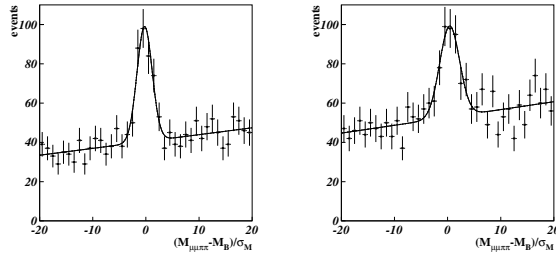


Figure 3: Signal for $B^0/\bar{B}^0 \rightarrow J/\psi K_s^0$. Horizontal axis is the normalized mass. *Left*: For the SVX sample, in which precision lifetime information is available. *Right*: For the non-SVX sample, in which no precision lifetime is available.

mass, vertex, and pointing constraints, and the resulting B^0/\bar{B}^0 candidate is required to have $p_T(B) > 4.5$ GeV. Quality cuts are applied to the vertex fit. Refit momentum and their errors are used to compute a normalized mass for the B^0/\bar{B}^0 candidate, defined as the deviation of the B^0/\bar{B}^0 candidate from the P.D.G value, divided by estimated error.

A silicon vertex detector(SVX) consisting of four layers of single sided silicon sensors provides precise impact parameter information for tracks falling within its acceptance. We divide the sample into two subsamples, one with precision silicon hits in both muons tracks (called the SVX sample) and one where at least one muon track lacks silicon hits (the non-SVX sample). From a fit to the normalized mass distribution in each of these subsamples (Fig. 3), we determine signal in the SVX and non-SVX samples to be 202 ± 18 and 193 ± 26 , respectively.

4 Initial state flavor tagging

Three algorithms are used to determine the initial state flavor (B^0 or \bar{B}^0) of the B meson decaying into $J/\psi K_s^0$.

- Same side tagging (SST) uses the correlations between the B^0/\bar{B}^0 and nearby hadrons to tag the flavor of the B^0/\bar{B}^0 . These correlations arise both from the decay of orbitally excited B mesons and from fragmentation.

Table 1: *Dilutions and efficiencies for the three tagging algorithms described in the text.*

tag type	efficiency	dilution
SST, SVX	35.5 ± 3.7	16.6 ± 2.2
SST, non-SVX	38.1 ± 3.9	17.4 ± 3.6
SLT	5.6 ± 1.8	62.5 ± 14.6
JETQ	40.2 ± 3.9	23.5 ± 6.9

- Opposite side jet-charge tagging (JETQ) tags the flavor of the B^0/\bar{B}^0 using an estimator of the charge of jet found in the opposite hemisphere.
- Soft lepton tagging (SLT) uses the sign of an soft (i.e. nontrigger) opposite-side μ^\pm or e^\pm to determine the flavor of the B^0 .

In the case of opposite-side tagging, the dilutions can be measured by tagging B^\pm reconstructed in the decay mode $B^0 \rightarrow J/\psi K^\pm$. About 1000 such events are reconstructed; they have the same kinematics as the signal events and therefore can be used to calibrate the tag. In the case of same-side tagging the situation is very different, since the dilution of the same sign tag is expected (and observed) to depend on the species of B meson. Instead, the SST dilution is measured using the semileptonic B decays, which enter the sample through a high- p_T semileptonic trigger ⁷). Asymmetries measured for charged and neutral modes are shown in Fig 4. The observed asymmetry is the product of a dilution and a *mixing* asymmetry, whose amplitude is $A_{mix} = 1.0$, and therefore the observed asymmetry measures directly the dilution of same side tagging. The p_T of the b -quark in this sample is higher than in the signal, and the dilution therefore larger. Monte Carlo is used to extrapolate to lower p_T .

Each of the three tagging algorithms has similar statistical power (about 2%), although they vary greatly in efficiency and dilution. Only about 40% of the jets on opposite the $B^0/\bar{B}^0 \rightarrow J/\psi K_s^0$ fall within the acceptance of the tracking detectors. Opposite side leptons suffer are further suppressed by semileptonic branching ratio. SST is very efficient, but has low dilution. SLT has high dilution but low efficiency. JETQ has moderate efficiency and moderately high dilution. The properties of these algorithms are shown in Table 1. The combined effective tagging efficiency is $6.3 \pm 1.7\%$.

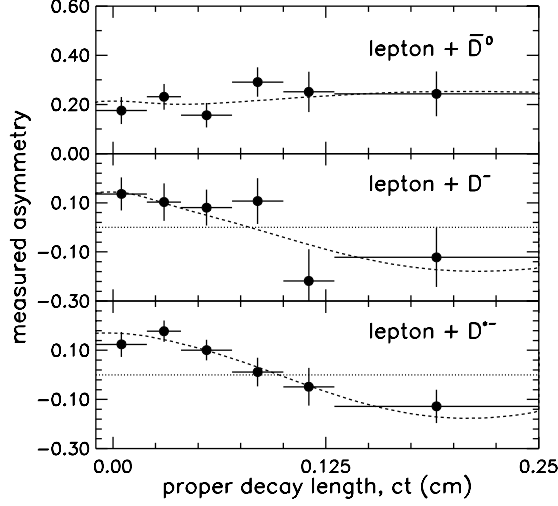


Figure 4: Same Side Tagging (SST). Mixing asymmetry vs. proper time is measured for three B decay channels: Lepton plus \bar{D}^0 (top) is a signature for B^+ : the asymmetry is flat with time. Lepton plus D^- (middle) and Lepton plus D^{*-} (bottom) are signatures of B^0 ; the asymmetry is cosine like and the amplitude gives the dilution of the tag.

The extraction of $\sin 2\beta$ is carried out using a trivariate unbinned maximum likelihood fit to the normalized mass, the decay time, and the tag pattern. Separate components in the fit describe the signal, the prompt background, and the long-lived background, each component being also a direct product of the time function, the mass function, and the tag function. Fit parameters are constrained where possible to the measured values (world average, or CDF measured) using Gaussian constraint terms. Parameters in the fit include the B lifetime τ_B , the mixing frequency Δm_d , scale factors for mass and decay time errors, efficiencies, and dilutions. Possible detector-related asymmetries in efficiency and dilution events are allowed in the fit, but tied by Gaussian constraints to average values measured in the calibration samples. More details on the fitting procedure can be found in the published reference ⁶).

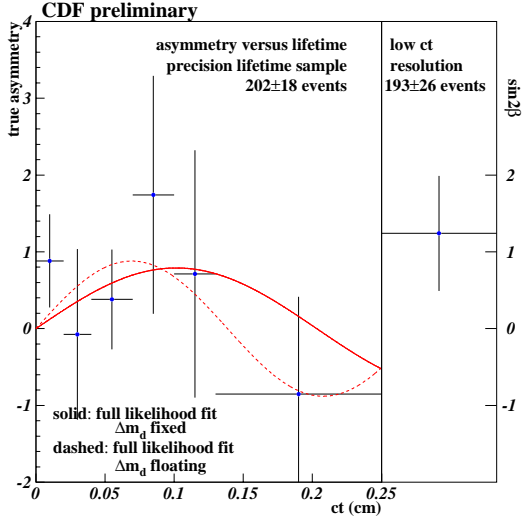


Figure 5: Fit to the $A_{cp}(t)$. Data points are asymmetries within six time bins (left) for the SVX sample, and in one inclusive bin (right) for the non SVX sample. The solid line is the fit with Δm_d constrained within errors to the world average value; the dashed line shows the fit with Δm_d floating.

The result, shown in Fig 5, yields $\sin 2\beta = 0.79^{+0.41}_{-0.44}$. The statistical error is 0.39, while the systematic error, dominated by the error in dilution, is 0.16. Table 2 shows the major sources of systematic error. When the fit is performed without constraining the mixing frequency Δm_d to its world average value of $0.472 \pm 0.017 \text{ ps}^{-1}$ (8), the fitter extracts $\sin 2\beta = 0.88^{+0.44}_{-0.41}$ and $\Delta m_d = 0.68 \pm 0.17 \text{ ps}^{-1}$, consistent with the world average at the level of $\approx 1.2\sigma$.

As a cross-check the three tagging algorithms are used to measure the mixing asymmetry in $B^0 \rightarrow J/\psi K^{0*}$, a flavor-specific decay. We reconstruct 226 ± 24 events with silicon hits on both muon tracks and 231 ± 28 events where at least one muon lacks silicon hits. Unbinned likelihood fits are performed, in which the A_{mix} is floating and Δm_d is fixed to the world average, and once again with Δm_d floating. Results are shown in Fig 6. The first fit measures $D = 1.0 \pm 0.37$, while the second fit measures $D = 0.96 \pm 0.38$ and $\Delta m_d =$

Table 2: Sources of systematic error in the $\sin 2\beta$ analysis.

Parameter	$\delta \sin 2\beta$	In fit
Dilution and Efficiency	.16	yes
Δm_d	negligible	yes
τ_B^0	negligible	yes
Trigger Bias	negligible	no
K_L^0 regeneration	negligible	no

$0.4 \pm 0.18 \text{ ps}^{-1}$. Both fits are consistent with expectations. The summary of direct measurements of CP asymmetry is shown in Fig. 7. CDF's precision is comparable at this point in time to the $\Upsilon(4S)$ experiments ^{3) 4)}. A weighted average including also the LEP results ^{12) 8)} yields $\sin 2\beta = 0.5 \pm 0.23$; one can compare this to a recent standard model fit of $\sin 2\beta = 0.75 \pm 0.09$ ⁹⁾. Informative as these plots are, one must keep in mind that the industry of precision CKM measurements in the B sector is still in its infancy. Much improvement is expected in the coming years from e^+e^- machines and from the Tevatron.

5 Run II upgrades

At CDF in Run II the improvements from both the accelerator, and also the detector. The accelerator which now operates with the main injector, is projected to deliver an instantaneous luminosity of $1.0 \times 10^{32} \text{ cm}^{-2}\text{s}^{-1}$ for an integrated luminosity of 2 fb^{-1} by the year 2003. This is to be compared with 110 pb^{-1} of luminosity integrated during Run I.

Upgrades to the detector include better particle identification, replacement of the silicon vertex detector (SVX) with a much larger 3D silicon tracking system; and the introduction of a displaced track trigger called the silicon vertex trigger or SVT that has the capability of triggering, for the first time, on hadronic decay modes such as $B^0/\bar{B}^0 \rightarrow \pi^+\pi^-$ and hadronic B_s^0 decays such as $B_s^0 \rightarrow D_s^- \pi^+$ with $D_s^- \rightarrow \phi\pi^-$.

The particle ID is relevant to B physics whenever flavor tagging is important; i.e. whenever mixing or CP asymmetries are measured. The new detector has better dE/dx in the tracking chamber plus a new time-of-flight system with resolution of 100 ps which together provide $K^\pm\pi^\pm$ separation of

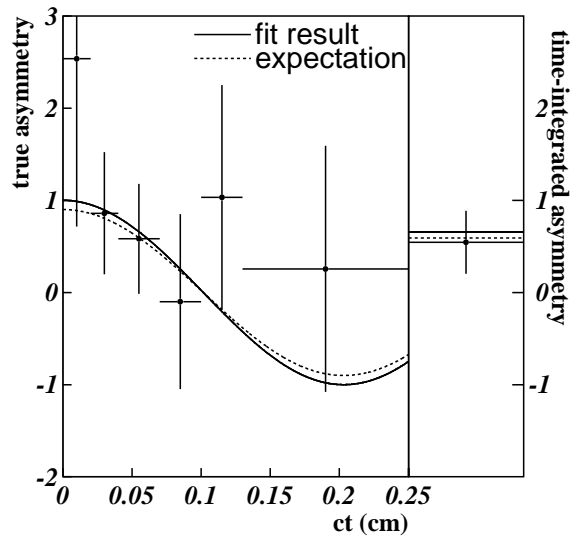


Figure 6: Mixing asymmetry in the decay $B^0 \rightarrow J/\psi K^{0*}$, using the same three taggers as in the $\sin 2\beta$ analysis. Data points are mixing asymmetries within six time bins (left) for the SVX sample and in one inclusive bin (right) for the non-SVX sample.

2σ for $p_T < 1.6$ GeV. This improves both same-side and opposite-side kaon tagging of B^0 and B_s^0 . Monte Carlo studies indicate that the effective tagging efficiency increases from 6.3% to 9.11% in B^0 events, and predict 11.3% tagging efficiency for B_s^0 .

The silicon upgrade replaces the two-barrel, four-layer 40,000 channel $r\phi$ -only SVX detector with a three-barrel, eight-layer, 750,000 channel double sided deadtimeless 3D precision silicon tracker. The tracker covers the angular region of $|\eta| < 2.0$; redundancy in this region gives the tracker standalone capabilities well past the $|\eta| < 1$ region covered by the tracking chamber. Precision information in z is generally expected to improve the signal-to-noise ratio of most B -physics signals. An extremely precise $r\phi$ -only innermost layer, mounted directly on the beampipe, gives a proper time resolution of $\sigma_{c\tau} \approx 0.03\tau_B$ for B decays.

Also in Run II, CDF has a track trigger at level one and the capability

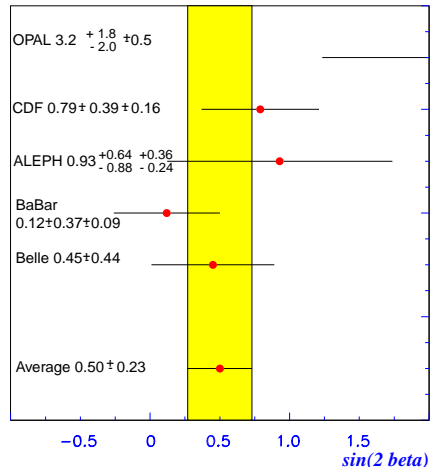


Figure 7: Comparison of results on $\sin 2\beta$ from summer 2000, from LEP, BaBar, Belle, and CDF, together with a weighted average.

of using impact parameter information from tracks in the level 2 decision. The displaced track trigger was operated for a short time during an October commissioning run with a crudely aligned single silicon barrel containing two ϕ wedges. The device operated according to expectations, achieving impact parameter resolutions of $87 \mu m$, as shown in Fig 8.

6 The Run II B physics program at CDF

The measurement of $\sin 2\beta$ using the decay channel $B^0/\bar{B}^0 \rightarrow J/\psi K_s^0$ in Run II will be performed much as in Run I; the expected event yield is derived from the run I yield, including the expected increase in integrated luminosity from the accelerator, the greater coverage of the SVXII detector and the lower muon trigger thresholds possible in run II thanks to the level one track trigger. We expect 10,000 events in run II using these gains alone. The effective tagging efficiency expected in Run II is 9.11%. Scaling the Run I result (both systematic and statistical errors scale with $1/\sqrt{N}$) gives an expected error of 0.072. Additional gains are possible from a dielectron trigger and from further improvements to muon triggers, or after a longer Tevatron Run.

Simultaneous measurement of A_{CP}^{dir} and A_{CP}^{mix} in $B^0/\bar{B}^0 \rightarrow \pi^+\pi^-$ and

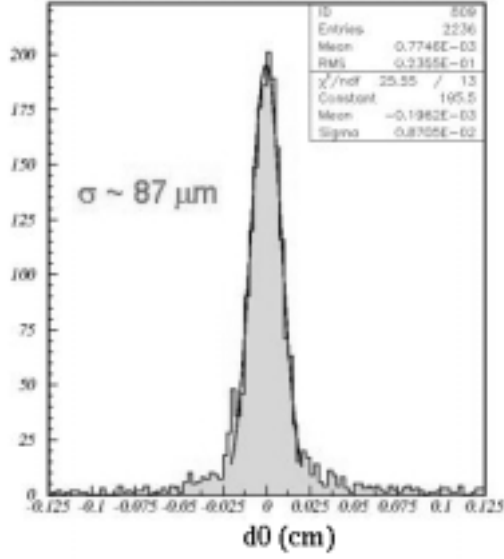


Figure 8: The beam profile in the commissioning run, measured with the (SVT). This device is the basis of our strategy to trigger on hadronic b -decays.

$B_s^0/\bar{B}_s^0 \rightarrow K^+K^-$ may constrain the CKM angle γ . In the limit of exact isospin symmetry in these decays, simultaneous measurement of these four observables determines β , γ , the magnitude of the ratio $d = P/T$ of penguin diagram to tree diagram, and the phase θ of this ratio¹⁰. The system of equations is:

$$A_{cp}^{mix}(B^0/\bar{B}^0 \rightarrow \pi^+\pi^-) = \sin 2(\beta + \gamma) + 2d \cos \theta (\cos \gamma \sin 2(\beta + \gamma) - \sin(2\beta + \gamma)) \quad (5)$$

$$A_{cp}^{dir}(B^0/\bar{B}^0 \rightarrow \pi^+\pi^-) = -2d \sin \theta \sin \gamma \quad (6)$$

$$A_{cp}^{mix}(B_s^0/\bar{B}_s^0 \rightarrow K^+K^-) = \frac{2\lambda^2}{d(1-\lambda^2)} \cos \theta \sin \gamma \quad (7)$$

$$A_{cp}^{dir}(B_s^0/\bar{B}_s^0 \rightarrow K^+K^-) = \frac{2\lambda^2}{d(1-\lambda^2)} \sin \theta \sin \gamma \quad (8)$$

These equations are degenerate if $\theta = 0$; however one can use the measurement of $\sin 2\beta$ from the $B^0/\bar{B}^0 \rightarrow J/\psi K_s^0$ to solve the system. Isospin symmetry

breaking affects this approach only insofar as *ratios* of penguin and tree matrix elements differ between the B^0 and B_s^0 system; which can be monitored by studying ratios of branching ratios $\frac{B(B^0 \rightarrow \pi^+ K^-)}{B(B_s^0/\bar{B}_s^0 \rightarrow K^+ K^-)}$ and $\frac{B(B^0/\bar{B}^0 \rightarrow \pi^+ \pi^-)}{B(B^0 \rightarrow \pi^+ K^-)}$, which do not depend on production rates. This type of investigation is unique to the Tevatron. It relies on the hadronic B trigger, and demands good particle identification and excellent proper time resolution in order to resolve two Fourier components (Δm_d and Δm_s) in the CP asymmetries.

Observation of $B_s^0 - \bar{B}_s^0$ flavor oscillations is expected in Run II. The proper time resolution $\sigma_{c\tau} \approx 0.03\tau_B$, ϵD^2 of 11.3%, event yields calculated to be of order 20,000, and signal to background ratios estimated from the data give estimates of the discovery potential of CDF for $B_s^0 - \bar{B}_s^0$ oscillations for x_s between 53 and 61, well above the standard model expectation.

Relating the mass difference in the B_s^0 system to that of the B^0 system determines the ratio of CKM matrix elements, free from many of theoretical uncertainties that the individual measurements suffer.

$$\frac{|V_{td}|}{|V_{ts}|} = 1.16 \pm 0.06 \sqrt{\frac{\Delta m_d M_{Bs}}{\Delta m_s M_{Bd}}} \quad (9)$$

The width difference between the heavy and light eigenstate can be related to the mass difference in a way which is free from CKM uncertainties (11):

$$\frac{\Delta\Gamma_s}{\Delta m_s} = -\frac{3}{2}\pi \frac{m_b^2}{m_t^2} \frac{\eta_{QCD}^{\Delta\Gamma}}{\eta_{QCD}^{\Delta m}} \quad (10)$$

This width difference, about 15% may be observable in the decay of $B_s^0/\bar{B}_s^0 \rightarrow \psi\phi$. The final state is a mixture of CP eigenstates, while the two mass eigenstates of B_s^0 are approximately CP pure. There is little CP violation in the decay, so each component has a distinct distribution in transversity angle as well as lifetime. In Run I CDF found a signal of 58 ± 12 events, which can be scaled to a Run II expectation of 4,000 events. Estimates of the precision in $\Delta\Gamma/\Gamma$ are obtained from Monte Carlo, using the signal-to-noise ratio from data and a CP fraction of 0.77 determined from Run I transversity analysis. We expect a precision $\sigma(\frac{\Delta\Gamma}{\Gamma}) = 0.052$ in run II.

7 Conclusions

The work of subjecting the CKM sector of the standard model to precision test is beginning to take place; studies of CP violation and $B_s^0 - \bar{B}_s^0$ oscillations are

particularly important for the program. Proton-antiproton experiments will make unique contributions because they will be a copious source of tagged B^0 and B_s^0 mesons, some of them fully reconstructed. The CDF experiment plans to measure the angle β through CP asymmetries in $B^0/\bar{B}^0 \rightarrow J/\psi K_s^0$, measure the right hand side of the triangle by observing $B_s^0 - \bar{B}_s^0$ oscillations, and has a plausible strategy for investigating the angle γ through measurement of A_{CP}^{mix} and A_{CP}^{dir} in $B^0/\bar{B}^0 \rightarrow \pi^+\pi^-$ and $B_s^0/\bar{B}_s^0 \rightarrow K^+K^-$.

8 Acknowledgements

The author thanks the organizing committee for an interesting and enjoyable workshop. This work was supported by DOE Grant DEFG0291ER40646.

References

1. J.H. Christenson *et al*, Phys. Rev. Lett. **13**, 138 (1964).
2. L. Wolfenstein, Phys Rev. Lett. **51**, 1945 (1983)
3. Francesca di Lodovico, *First Physics results at BaBar*, these proceedings.
4. Masa Yamauchi, *First Results from Belle*, these proceedings.
5. F. Abe *et. al.*, Nucl. Instrum. Meth. **A271**, 387 (1988); F. Abe *et. al.*, Phys. Rev. **D 50** 2966 (1994); P. Azzi *et. al*, Nucl. Instrum. Meth. **A 260**, 137 (1995)
6. T. Affolder *et. al.*, Phys. Rev. **D 61**, 072005 (2000)
7. F.Abe *et. al.*, Phys. Rev. Lett. **80** 2057 (1998), Phys. Rev. **D 59**, 032001 (1999), P. Maksimovic'c, Ph.D. Thesis, Massachusetts Institute of Technology 1998.
8. C. Caso et al, The Eur. Phys. J. **C 15** (1998)
9. S. Mele, Phys. Rev. **D 59**, 113011 (1999)
10. R. Fleischer, Phys. Lett **B 469**, 306 (1999)
11. Isard Dunietz, Phys. Rev. **D 52**, 3048-3064 (1995)
12. K. Ackerstaff *et. al.*, Z. Phys. **C 76**, 401 (1997)